Investigating the effects of Carbon and Boron atoms on the τ-MnAl alloy properties employing the first principle approach

ID Sebe[1*], ME Sithole[1] and R Modiba[2]

[1]Department of Physics, Sefako Makgatho Health Science University, P.O. Box 94, Medunsa, 0204, South Africa.
[2]Materials Science and Manufacturing, CSIR, P.O. Box 395, Pretoria, 0001, South Africa.

[*]E-mail: **itumelengsebe16@gmail.com**

Abstract. Permanent magnet-based technologies are focusing on the use of τ-phase magnetic alloys. The τ-MnAl permanent magnetic alloys are interesting candidates to fill the performance gap between the expensive rare-earth-based magnets and the low performance ferrites. The purpose of the study was to investigate the effects of carbon and boron on the structural, electronic and magnetic properties of τ-MnAl using the first principle method. The first principle calculations were performed using the density functional theory (DFT) within the generalized gradient approximation (GGA), with the perdew-burke-eruzer (PBE) function for exchange-correlation potential employed in CASTEP to study the electronic, and magnetic properties of τ-MnAl magnets. The study revealed that τ-MnAl have a total magnetic moment of $3.04\mu_B$, where Mn and Al have $2.69\mu_B$ and $0.35\mu_B$ respectively. A decrease in magnetic moment of Mn from $2.69\mu_B$ to $1.51\mu_B$ was obtained adding B atoms. The DOS of τ-MnAl was observed to have a lower peak at the fermi level. The magnetic moment obtained for Mn was $0.46\mu_B$ after C atoms were added. The DOS of Mn_3AlC shifted to the right with the highest peak at the fermi level. The results obtained revealed that the DOS of τ-Mn_2AlB_2 and τ-Mn_3AlC have their highest peaks at the fermi level. This was due to the decrease in magnetic moment of Mn after adding C and B to τ-MnAl.

1. Introduction

Permanent magnets are an essential component of modern life, where their use in technology is still expanding. They are the basic building blocks of various electromechanical and electrical devices. Based on the requirements for the various applications of permanent magnets, such as the strength of the magnet for a given size, the ability of the magnet to maintain its field in the presence of a reverse field, high temperatures, and hostile environments, as well as its cost [1]. Various energy-efficient appliances, direct-drive wind turbines, hybrid and electric motors, and wind turbines all contain significant amounts of permanent magnets. Due to their outstanding magnetic properties, rare earth magnets like Dy-substituted $Nd_2Fe_{14}B$, $SmCo_5$, and $Sm_2Fe_{17}N$ have been employed in all these devices. Nd, Sm and Dy, however, are becoming more expensive. As a result, creating powerful permanent magnets without rare earth elements is a growing concern [2].

Due to their significant advantages, such as high saturation magnetization, large theoretical $(BH)_{max}$, decent Curie temperature and extremely low cost. The tetragonal phase (τ-phase) MnAl permanent magnetic alloys are an interesting candidate to close the performance gap between the expensive rare-earth-based magnets and the low performance ferrites [3]. The τ-phase (tetragonal $L1_0$ superstructure, space group of P4/mmm) is the sole ferromagnetic phase in the MnAl binary system and

it is thermodynamically metastable [3]. This study aims to investigate the structural, magnetic, and electronic properties of τ-MnAl alloys employing the first principle method.

2. Methodology

The Cambridge Sequence Total Energy Package (CASTEP) code and the Generalized Gradient Approximation in the Perdew-Burke-Eruzer (PBE) scheme were used in this study. The structural, electronic, and magnetic properties of the τ-MnAl unit cell were calculated. We performed geometry optimization before calculations of τ-MnAl properties and in all calculations spin-polarization was considered [4]. The convergence criterion for structure optimization and energy calculations was set to a fine quality. The experimental MnAl lattice parameter (a=3.93 and c=3.56) with the atomic radii (1.43Å for Al and 1.26Å for Mn) and energy convergence of 10^{-6} were utilized in all calculations. The tolerance for the stress concentration factor (SCF), energy, maximum force, and maximum displacement was set to eV/atom, eV/atom, 0.03, and 0.001 respectively for all calculations. The Brillouin-zone (BZ) integration Pack has been used with a 700eV energy cut-off and 9×9×7 Monkhorst-Pack *k*-point grids [5].

3. Results and discussion

3.1. Structural and Magnetic Properties of τ-MnAl

Fig 1 shows simulated crystal structure of τ-MnAl. This is a metastable τ-phase MnAl tetragonal $L1_0$ superstructure, with a space group of P4/mmm. The τ-MnAl structure is composed of 5 atoms (1 Mn and 4 Al atoms). The structure went through full geometry optimization. When the energy was at its lowest after optimization the cell was at its most stable states [4].

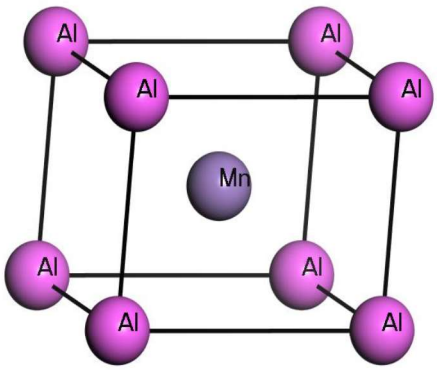

Figure 1. The crystal structure of τ-MnAl.

Table 1, shows the calculated lattice parameters of the τ-MnAl structure. The calculated c/a ratio with respect to pure τ-MnAl doped with C and B were 1.271Å, 1Å and 0.495Å which is close to that obtained in previous study [6]. When B and C atoms were added in τ-MnAl, the increase in lattice parameters was observed.

Table 1. Lattice parameters of τ-MnAl Structures.

Structures	a (Å)	b (Å)	c (Å)	c/a (Å)
τ-MnAl	2.753	2.753	3.500	1.271
τ-Mn_2AlB_2	5.727	5.727	2.834	0.495
τ-Mn_3AlC	3.807	3.807	3.807	1.0

Table 2. shows the calculated total magnetic moments of τ-MnAl structures. The magnetic moments of Mn and Al together equal 3.04μ_B, while Mn and Al alone had 2.69μ_B and 0.35μ_B, respectively. After B and C atoms were added, the magnetic moment of Mn decreases to 1.5μ_B and 0.46μ_B respectively. The positive and negative moments of Mn and Al atoms after adding C and B indicate antiferromagnetic coupling between their sublattice.

Table 2. The total magnetic moments of structures.

STRUCTURES	Mn(μ_B)	Al(μ_B)	B(μ_B)	C(μ_B)	Total(μ_B)
τ-MnAl	2.69	0.35	-	-	3.04
τ-Mn_2AlB_2	1.51	-0.24	-0.17	-	1.1
τ-Mn_3AlC	0.46	-0.03	-	-0.04	0.39

3.2 Electronic Properties

3.2.1 Density of states

The density of states (DOS) of doped (C and B) and undoped τ-MnAl structures is shown in Fig 2. The instability of the structure is related to the Fermi level (E_f), represented by the vertical line in Fig 2. Structures with the highest DOS at E_f are considered the least stable, whereas the lowest are the most stable [7]. The DOS of τ-MnAl has its highest peak just before it reaches the Fermi level and is at its lowest peak when is at the fermi level which is antiferromagnetic. This is due to the high magnetic moment of Mn 2.69μ_B. The addition of carbon lowers the magnetic moment of Mn from 2.69μ_B to 0.46μ_B. The DOS of τ-Mn_3AlC is at its highest peak just as it approaches the Fermi level and a bit low but above that of τ-MnAl at the Fermi level. The τ-Mn_2AlB_2 DOS is above both τ-MnAl and τ-Mn_3AlC DOS from the range -15eV to 18eV, except that it has a lower τ-Mn_3AlC peak when approaching the Fermi level.

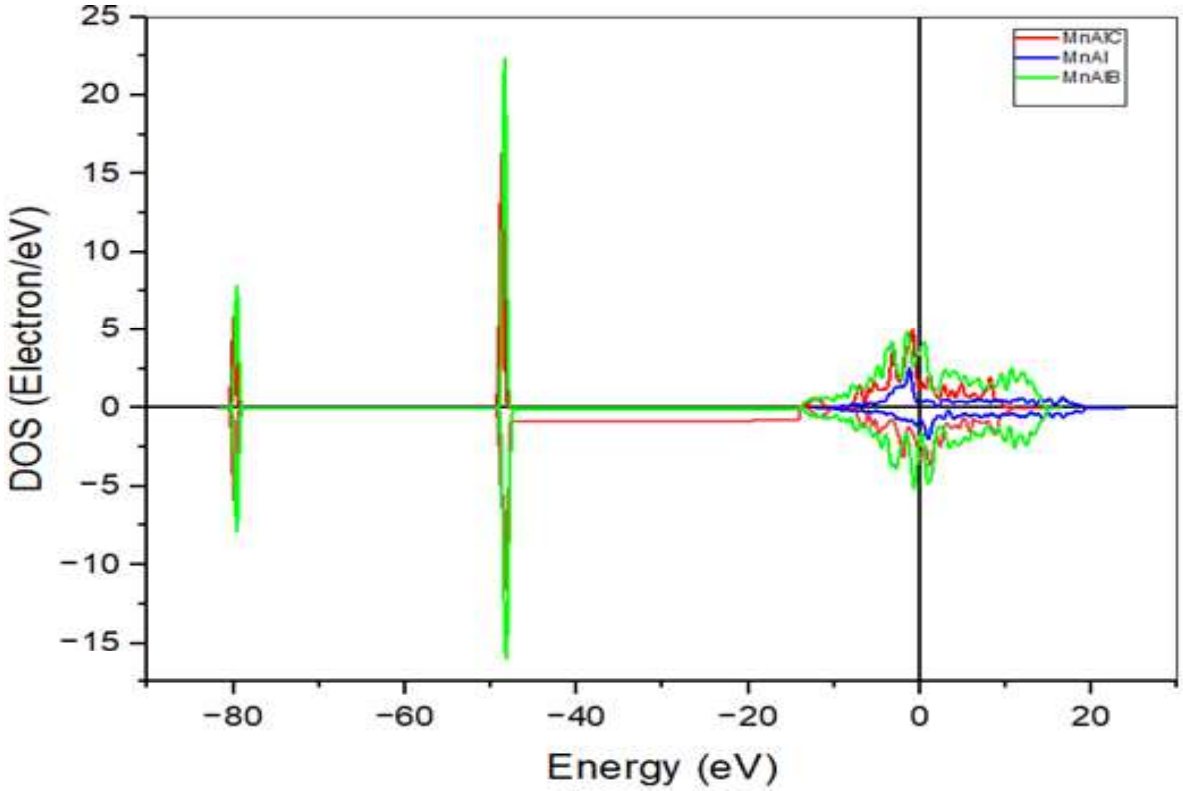

Figure 2. Comparison of the total density of states (DOS) for τ-MnAl doped with C and B structures. $E_F = E = 0$.

4. Conclusion

In conclusion, the τ-MnAl structure was optimized using first principles PBE-GGA calculations. The electronic and magnetic properties, including lattice constants, densities of states, and magnetic moment, were examined. Due to the expansion of the crystal lattice caused by the inclusion of the carbon and boron atoms, the c/a ratio decreased. The τ-MnAl doped with carbon seem to be the most stable since it has the lowest DOS at the Fermi level ($E_f = 0$). Boron doped structure is the least stable since its DOS is the highest at Fermi level.

Acknowledgements

The authors thank Sefako Makgatho Health Science University and NRF for their financial support. The support from the CSIR is highly recognised. The calculations were performed using the computers of the high-performance computing centre (CHPC) in Cape Town.

References

[1] McCallum R W, Lewis L, Skomski R, Kramer M J and Anderson I E 2014 Practical aspects of modern and future permanent magnets *Annu. Rev. Mater. Res.* **44** 451-77

[2] Park J H, Hong Y K, Bae S, Lee J J, Jalli J, Abo G S, Neveu N, Kim S G, Choi C J and Lee J G 2010 Saturation magnetization and crystalline anisotropy calculations for MnAl permanent magnet *J. Appl. Phys.* **107** 1-5.

[3] Zhao S, Wu Y, Wang J, Jia Y, Zhang T and Jiang C 2019 Realization of large coercivity in MnAl permanent magnet alloys by introducing nanoprecipitates *J. Magn. Mater.* **483** 164-68.

[4] Yang J, Xiao Z, Wen Q and Yang F 2014 First principle study on the structural, electronic and magnetic properties of Ni_4C *Compu. Conde. Matt.* **1** 51-57.

[5] Miya L E and Sithole M E 2022 Investigating the electronic and magnetic properties of Dy, Y and La by site substitution on $Nd_2Fe_{14}B$ permanent magnet employing the first-principle approach *Conf. SA Advan. Mater. Init.* **40** 224-227.

[6] Kontos S, Fang H, Li J, Delczeg-Czirjak E K, Shafeie S, Svedlindh P, Sahlberg M and Gunnarsson K 2019 Measured and calculated properties of B-doped τ-phase MnAl *J. Magn. Mater.* **474** 591-598.

[7] Mahlangu R, Phasha M J, Chauke H R, Ngoepe P E 2013 Structural, elastic, and electronic properties of equiatomic PtTi as potential high-temperature shape memory alloy *Intermetallics.* **33** 27-32.